

# A Convenient Approach for Preparation of Cu-Ag Alloy Particles Using Hyperbranched Polymers as Templates

Han Wensong

*Institute of Advanced Energy Materials and Chemistry, Qilu University of Technology (Shandong Academy of Sciences), Jinan 250353, China*

**Abstract:** Cu-Ag particles with different molar ratios have been prepared in the hyperbranched polyester matrix using ascorbic acid as a reducing agent. The third generation hyperbranched polyester has been synthesized by step by step polymerization using the first generation hyperbranched polyester as core molecular and 2, 2-dimethylol propionic acid as branched monomer. The synthesized hyperbranched polyester and Cu-Ag alloy were characterized by FT-IR, <sup>1</sup>H-NMR, UV-vis spectra, X-ray diffraction (XRD), SEM, Energy Dispersive X-ray (EDX), Laser particle size measurement, TEM, etc. The XRD and EDX studies confirm the formation of Cu-Ag alloy. Laser particle size measurement, SEM and TEM studies show that the particles of the Cu-Ag alloy are well-dispersed with average size of 120 nm. The thermal properties of the Cu-Ag alloy have been studied by thermogravimetric Analysis (TGA). The results show that the measurement values are close to the theoretical ones.

**Key words:** rare metal; Cu-Ag alloy; hyperbranched polyester; synthesis

In recent years, silver and copper nanoparticles have received much attention due to their high electrical conductivity<sup>[1-4]</sup>. Because of the rare content of silver in earth and easy oxidization of copper, their application is restricted. Formation of Cu-Ag alloy nanoparticles instead of single copper or silver particles is considered to be an advisable option to solve above problems. Preparation of such nanoparticles required the use of dispersants which prevent the aggregation of the nanoparticles in solution<sup>[5-8]</sup>.

Hyperbranched polymers have gained widespread attention due to their globular shape, highly branched topology, and a large number of end groups<sup>[9-12]</sup>. These specific structural features give hyperbranched polymers different properties compared to linear analogues of equivalent molar masses. In contrast to dendrimers, hyperbranched polymers could be synthesized in one step from  $AB_n$  ( $n \geq 2$ ) type monomers and could be used in many fields<sup>[13-18]</sup>. Singh et al<sup>[19]</sup> synthesized silver nanoparticle in a hyperbranched polyamine matrix by a reductive. Wan et al<sup>[20]</sup> synthesized gold nanoparticles using amphiphilic hyperbranched polyglycerol polymers as a template. Li and Luo<sup>[21]</sup> prepared Cu-Ag bimetallic nanoclusters using

PAMAM dendrimers as an outer template and a dispersant. Although a lot of work has been done on the preparation of monometallic nanoparticles, there are only a few reports on Cu-Ag nanoparticles using hyperbranched polymers as templates and dispersants.

Here, we report the synthesis and characterization of Cu-Ag nanoparticles. These Cu-Ag nanoparticles are prepared using ascorbic acid as a reducing agent and the third-generation hyperbranched polyester as templates. The chemical structures of the different generation hyperbranched polyester were characterized by FT-IR and <sup>1</sup>H-NMR. The Cu-Ag nanoparticles with different molar ratios were characterized by UV-vis spectra, XRD, EDX, TEM, etc. These prepared Cu-Ag nanoparticles have narrow size distribution and potential application in many fields.

## 1 Experiment

### 1.1 Materials

Pentaerythritol triacrylate (PETA), ethylenediamine and 2, 2-Dimethylol propionic acid (DMPA) were purchased from Aladdin Reagent Co. (Shanghai, China). Silver nitrate

Received date: May 25, 2017

Corresponding author: Han Wensong, Ph. D., Institute of Advanced Energy Materials and Chemistry, School of Chemistry and Pharmaceutical Engineering, Qilu University of Technology, Jinan 250353, P. R China, E-mail: [hws0633@163.com](mailto:hws0633@163.com)

Copyright © 2018, Northwest Institute for Nonferrous Metal Research. Published by Elsevier BV. All rights reserved.

(AgNO<sub>3</sub>, 99.9%), copper nitrate (Cu(NO<sub>3</sub>)<sub>2</sub>·3H<sub>2</sub>O, 99.5%) and ascorbic acid were obtained from Sinopharm Chemical Reagent Co. Ltd, China. Dimethylacetamide, p-toluenesulfonic acid (*p*-TSA), Gun Arabic, ethyl ether, ethanol, ammonia water and acetone were purchased from Lingfeng Chemical Reagent Co. Ltd. (Shanghai, China). All of these chemicals were used as received without further purification.

## 1.2 Synthesis of water-soluble first-generation hyperbranched polyester (HBPE-1)

PETEA (3.520 g, 0.01 mol), DEA (4.206 g, 0.04 mol) and methanol (30 mL) were charged into a 150 mL three-necked flask equipped with a magnetic stirrer, nitrogen inlet and a cooler. The mixture was stirred for 36 h at 40 °C under nitrogen atmosphere. After cooling to room temperature, the white precipitate was filtrated, washed with methanol and dried under vacuum for 24 h. The water-soluble first-generation hyperbranched poly (ester amine) was obtained (yield: 6.026 g, 78%). The synthesis process is described in Fig. 1.

IR (KBr, cm<sup>-1</sup>): 3327.4 cm<sup>-1</sup> ν(-OH), 2886.2~2955.7 cm<sup>-1</sup> ν(-C-H stretching vibration), 1724.9 cm<sup>-1</sup> ν(-C=O), 1452.1 cm<sup>-1</sup> ν(-C-N-), 1126.9 and 1042.1 cm<sup>-1</sup> ν(-C-O), 871.6 cm<sup>-1</sup> ν(-C-H deformation vibration). <sup>1</sup>H-NMR (DMSO-*d*<sub>6</sub>, 10<sup>-6</sup>): 4.16~4.18 (-C-CH<sub>2</sub>-O-), 3.31~3.35 (-CH<sub>2</sub>-OH, -CH<sub>2</sub>-N<), and 2.48~2.51 (-OOC-CH<sub>2</sub>, -N-CH<sub>2</sub>-).

## 1.3 Synthesis of water-soluble third-generation hyperbranched polyester (HBPE-3)

The water-soluble third-generation hyperbranched polyester was synthesized by step by step polymerization technique using HBPE-1 as core molecular and DMPA as branched monomer. The details of the synthetic method for HBPE-3 are described as follows: HBPE-1 (0.7726 g, 1 mmol), DMPA (3.219 g, 24 mmol), 0.10 g *P*-TSA and 30 mL *N*-methyl-2-pyrrolidone as solvent were added to a three-necked round-bottomed flask, which was equipped with a thermometer, nitrogen inlet and Dean-stark apparatus. The reaction mixture was stirred for 6 h at 140 °C under nitrogen atmosphere. The eliminated water was collected

from the Dean-Stark apparatus. After cooling to room temperature, the reaction mixture was poured into cyclohexane. The precipitate was collected and dried under vacuum to give a yellow viscous fluid (yield: 2.918 g, 82%). The synthesis process is described in Fig. 2.

IR (KBr, cm<sup>-1</sup>): 3389.1 cm<sup>-1</sup> ν(-OH), 2843.1~2916.7 cm<sup>-1</sup> ν(-C-H stretching vibration), 1719.1 cm<sup>-1</sup> ν(-C=O), 1459.1 cm<sup>-1</sup> ν(-C-N-), 1139.7 cm<sup>-1</sup> ν(-C-O), 1042.7 cm<sup>-1</sup> ν(C-O asymmetric stretching) 872.1 cm<sup>-1</sup> ν(-C-H deformation vibration). <sup>1</sup>H-NMR (DMSO-*d*<sub>6</sub>, 10<sup>-6</sup>): 4.61 (-CH<sub>2</sub>OOC), 3.87~4.06 (-C-CH<sub>2</sub>-O-), 3.33~3.51 (-CH<sub>2</sub>-OH, -CH<sub>2</sub>-N<), 2.55 (-OOC-CH<sub>2</sub>, -N-CH<sub>2</sub>-), and 0.90~1.05 (-CH<sub>3</sub>).

## 1.4 Preparation of Cu-Ag alloy nanoparticles using hyperbranched polymers as templates

The Cu-Ag alloy nanoparticles were prepared using ascorbic acid as a reducing agent and the third-generation hyperbranched polyester as templates. One typical process for synthesizing Cu-Ag (1:1) alloy nanoparticles was described as follows: 50 mL silver nitrate solution (0.01 mol/L), 50 mL copper nitrate solution (0.01 mol/L) and 1% (w/v) third-generation hyperbranched polyester aqueous solution were mixed together to produce a reaction mixture. 100 mL ascorbic acid aqueous solution (0.01 mol/L) was slowly added into the mixture at 70 °C. The change in color of the solution indicated the formation of the Cu-Ag alloy nanoparticles. Then, centrifuging gave a brown precipitates. The precipitates were washed with water and alcohol and then dried under vacuum. Similarly, using the same methods, the Cu-Ag (3:1), Cu-Ag (1:3), pure Ag and pure copper were prepared. The synthesis process is described in Fig. 3.

## 1.5 Measurement

The chemical structures of the hyperbranched polyester were measured by Infrared Absorption Spectra (Nicolet Magna IR650; Nicolet Analytical Instruments, Madison, WI) and <sup>1</sup>H-NMR with a Bruker 500 MHz spectrometer (Karlsruhe, Germany). The UV spectra were measured with UV-vis spectrophotometer (Simadzu UV-2450, Japan).

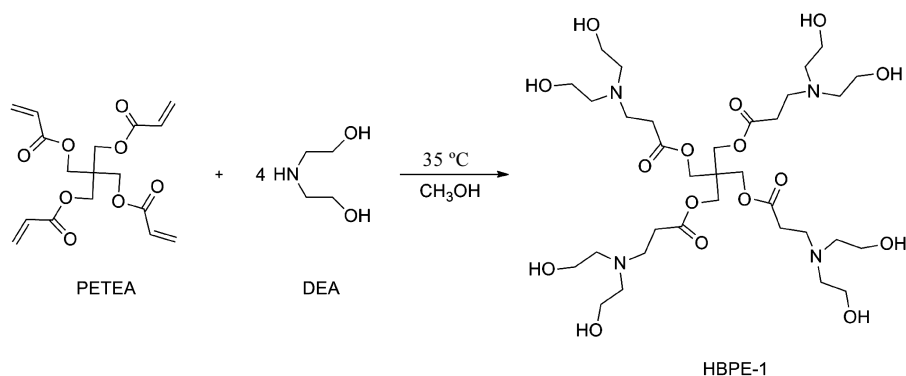


Fig. 1 Synthesis of first-generation hyperbranched polyester

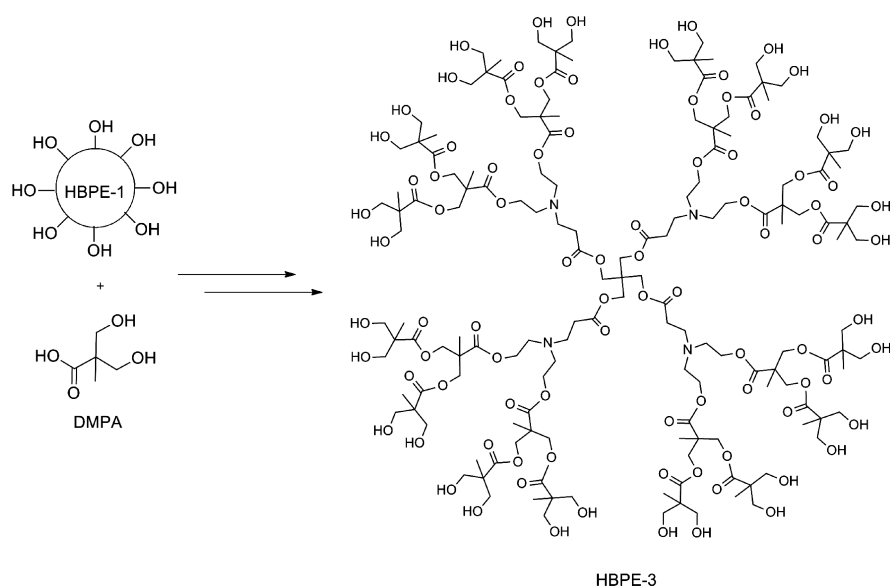


Fig.2 Synthesis of the third-generation hyperbranched polyester

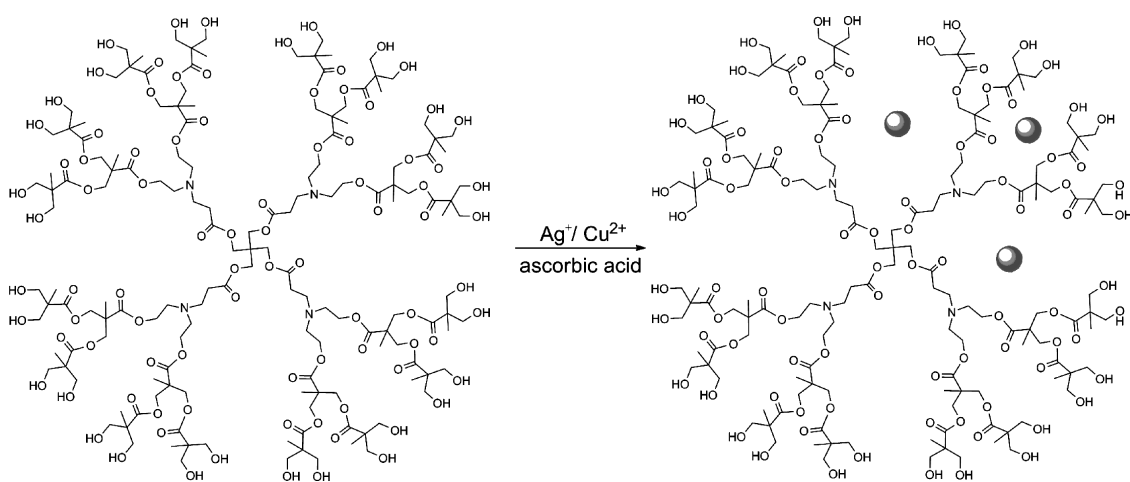


Fig.3 Preparation of Cu-Ag alloy nanoparticles using hyperbranched polymers as templates

X-ray diffraction measurements were performed on a D/max-III A X-ray diffractometer (Rigaku Denki, Tokyo, Japan). The particle size and its distribution were measured by laser light scattering. Transmission electron microscopy (TEM) micrographs were obtained with a JEM 1400 transmission electron microscope operated at an accelerating voltage of 120 kV. TGA spectra were recorded on a TA Instruments Q20 instrument (New Castle, DE) under air purge at a heating rate of 20 °C/min.

## 2 Results and Discussion

### 2.1 FT-IR and $^1\text{H}$ -NMR

The first generation hyperbranched polyester (HBPE-1) was synthesized by the Michael addition reaction of PETEA and DEA. Then the third generation hyperbranched polyester

was synthesized by a step by step polymerization approach using HBPE-1 as a core molecular and DMPA as branched monomer. Fig. 4 shows the FT-IR spectra of HBPE-1 and HBPE-3. A strong and broad peak around 3389.1  $\text{cm}^{-1}$  confirms high concentration of hydroxyl groups in hyperbranched polyesters. The peaks at around 2955.8  $\text{cm}^{-1}$  are assigned to the stretching vibration of  $-\text{CH}_2$  and  $-\text{CH}_3$ . The peaks at 1719.1 and 1422.8  $\text{cm}^{-1}$  are assigned to the stretching vibrations of N-C and C=O groups, respectively. The characteristic peaks of ester group are observed at 1130.7 and 1035.7  $\text{cm}^{-1}$ , indicating the esterification reaction has taken place<sup>[22, 23]</sup>. The  $^1\text{H}$ -NMR spectra of HBPE-1 and HBPE-3 are shown in Fig. 5. From the  $^1\text{H}$ -NMR spectrum of HBPE-1 (Fig. 5a), the proton signals at  $4.16 \times 10^{-6} \sim 4.18 \times 10^{-6}$  ( $-\text{C}-\text{CH}_2-\text{O}-$ ),  $3.31 \times 10^{-6} \sim 3.35 \times 10^{-6}$  ( $-\text{CH}_2-\text{OH}$ ,  $-\text{CH}_2-\text{N}<$ ), and

2.48~2.51 ( $-\text{OOC}-\text{CH}_2-$ ,  $-\text{N}-\text{CH}_2-$ ) are observed. After esterification, the peaks at about  $1.02 \times 10^{-6}$  and  $4.39 \times 10^{-6}$  which belong to the methyl and methylene groups of DMPA are clearly visualized in Fig.5b. This indicates that the DMPA has reacted with HBPE-1. From above analysis, it can be concluded that the HBPE-3 has been successfully synthesized<sup>[24]</sup>.

## 2.2 UV-vis spectra

The formation of Cu-Ag alloy in hyperbranched polymer matrix is observed by UV-vis absorption spectrum. Fig.6 shows a series of UV-vis spectra of nanoparticles made with various Cu/Ag ratios. It can be seen that the UV-vis spectra

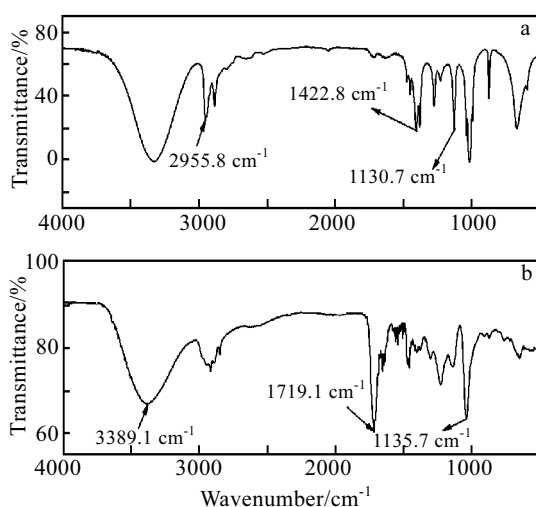


Fig.4 FT-IR spectra of HBPE-1 (a) and HBPE-3 (b)

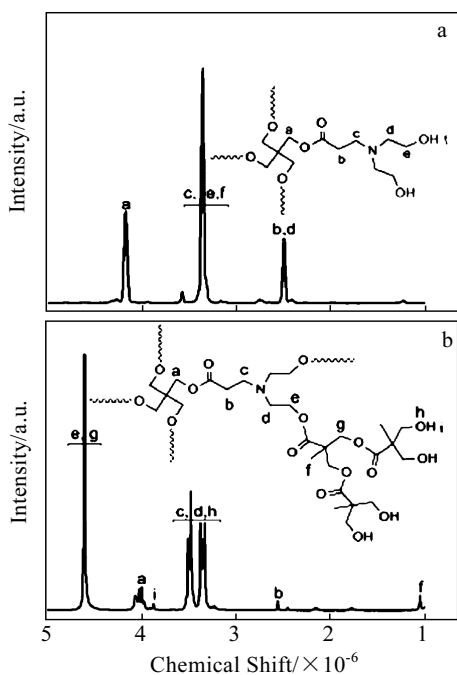


Fig.5  $^1\text{H}$ -NMR spectra of HBPE-1 (a) and HBPE-3 (b)

vary greatly depending on the Cu/Ag ratios. There is a strong absorption at about 420 nm after reduction of  $\text{Ag}^+$  ions to Ag (Fig.6a). This peak is due to the surface plasmon absorption of silver nanoparticles. It is well known that the Ag nanoparticles exhibit intense Plasmon absorption band in this visible region<sup>[25]</sup>. The Cu nanoparticles show no absorption band at about 420 nm (Fig.6e). For the Cu-Ag alloy nanoparticles, the Plasmon band appear between the two and the Plasmon absorption bands become weak with increasing the proportion of copper (Fig.6b~6d). It can also be seen that there is a single absorption band for the Cu-Ag alloy (1:3, 1:1, 3:1), indicating the Cu-Ag particles are in alloy form rather than a mixture of individual metal particles<sup>[26]</sup>.

## 2.3 Cu-Ag alloy particles size

The Ag, Cu, and Cu-Ag alloy nanoparticles could be synthesized in aqueous matrix of hyperbranched polyester. Ag nanoparticles could be synthesized at room temperature, while the Cu nanoparticles must be synthesized at about 70  $^{\circ}\text{C}$ . This is because the standard electrode potential of  $\text{Cu}^{2+}/\text{Cu}^0$  and  $\text{Ag}^+/\text{Ag}$  is different. Cu-Ag alloy nanoparticles are obtained by the simultaneous reduction of copper (II) nitrate hydrate and silver nitrate in hyperbranched polyester at 70  $^{\circ}\text{C}$ . The optical properties of these nanoparticles vary with the Cu/Ag molar ratio, which can be seen from the digital photographs in Fig. 7A. The color of silver and copper sol is yellow and brown, respectively (Fig.7A-a~e), while the color of Cu-Ag alloy is between them (Fig.7A-b~d). The change of color indicates the formation of Cu-Ag alloy nanoparticles. Fig.7B shows the particle size distribution of Ag, Cu-Ag (1:1) and Cu. It can be seen that the nanoparticles are in the range of 119.3~202.7 nm in diameter with narrow size distribution<sup>[27]</sup>. Pure Ag has a smaller particle size than pure Cu, as shown in Fig. 7B-a~c. Fig. 7B-b shows the particle size distribution of Cu-Ag (1:1). It can be seen that the Cu-Ag (1:1) also exhibits

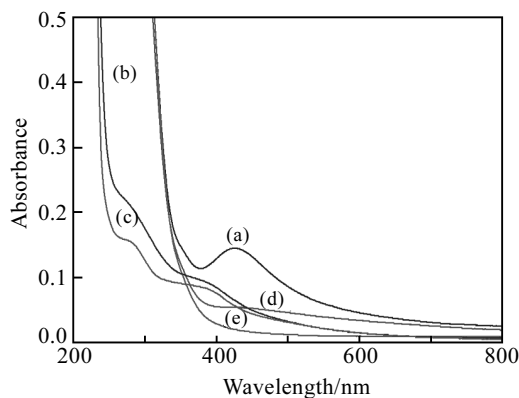


Fig.6 UV-vis absorption spectra of Cu-Ag alloy nanoparticles with various Cu/Ag ratios (the Ag/Cu mole ratios: a-1:0, b-3:1, c-1:1, d-1:3, and e-0:1)

narrow distribution and the particle size of it is larger than that of pure Cu and Ag. This may be due to the difference of the nucleation rate<sup>[28]</sup>.

## 2.4 X-ray diffraction analysis

X-ray diffraction (XRD) analysis was carried out on prepared nanoparticles. Fig.8 shows the XRD patterns of Cu, Ag and Cu-Ag alloy with different mole ratios. In Fig. 8a and 8b, the pure Cu and Ag are detected: Cu (111) orientation at  $43.1^\circ$ , Cu (200) at  $50.5^\circ$ , Cu (220) at  $74.1^\circ$  and Ag (111) orientation at  $38.1^\circ$ , Ag (2 0 0) at  $44.2^\circ$ , Ag (220) at  $64.4^\circ$ , Ag (311) at  $77.4^\circ$ . All the prominent peaks are in good agreement with the standard data of Cu and Ag. Fig. 8c–8e show the XRD patterns of Cu-Ag alloy nanoparticles. It can be seen that both Cu and Ag characteristic peaks are detected. Moreover, with the increase of silver content, the characteristic peaks of copper are decreased and the characteristic peaks of silver are increased. From above analysis, it can be concluded that the Cu-Ag alloy nanoparticles are successfully synthesized<sup>[29, 30]</sup>.

## 2.5 SEM-EDX analysis

There are many factors affecting the size of the Cu-Ag alloy, such as the structure of the hyperbranched polymer,

pH, the mole ratio of  $\text{Cu}(\text{NO}_3)_2/\text{AgNO}_3$  and the amount of  $\text{Cu}(\text{NO}_3)_2$  or  $\text{AgNO}_3$ . Fig.9a~9c show the SEM images of Cu-Ag alloy. It can be seen that the Cu-Ag alloy has similar structure, with the diameter around 120 nm. The element composition of the Cu-Ag alloy was also investigated by EDX, as shown in Fig.9d–9f. It can be seen that the Cu, Ag signals are all observed in the Cu-Ag alloy. With a decrease in the Cu/Ag molar ratio from 3:1 to 1:3, the Cu peaks decrease. From above analysis, it can be concluded that the Cu-Ag bimetallic particles are successfully formed at the atomic level<sup>[31, 32]</sup>.

## 2.6 TEM analysis

The structure of the Cu-Ag (1:1) was also studied by TEM and the results are shown in Fig.10. An aqueous Cu-Ag (1:1) was dropped on a copper grid and the sample was then dried under vacuum oven and subsequently imaged. Fig. 10a displays the TEM image of Cu-Ag (1:1) alloy. It can be seen that the particles size of the Cu-Ag alloy is around 120 nm. The result is in agreement with the laser particle-size distribution measurement. Fig.10b shows the selected area electron diffraction pattern of Cu-Ag alloy. Cu and Ag characteristic peaks are both present in the particles after reduction, which indicates the formation of Cu-Ag alloy. This result is also consistent with XRD studies.

## 2.7 TGA analysis

TGA is one of the most widely used techniques for the thermal stability evaluation of the mental nanoparticles. The TGA curves of Cu, Cu-Ag alloy and Ag nanoparticles are shown in Fig. 11. It can be seen that the Cu and Cu-Ag alloy have obvious increasing parts. They are attributed the oxidation of copper. For pure Cu, there is about 24.1% increase in mass (Fig.11a). The measured result is close to the theoretical vale of 25.2%. This indicated that the copper is completely oxidized into copper oxide at high temperature<sup>[33]</sup>. The increment of the mass for Cu-Ag (3:1), Cu-Ag (1:1) and Cu-Ag (1:3) are 118.6, 113.2 and 107.5%,

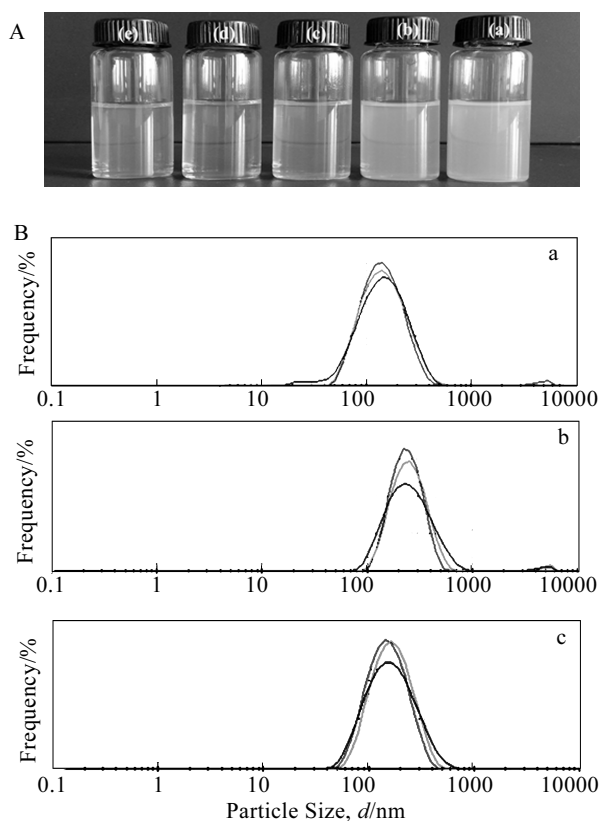


Fig.7 Digital photograph of metallic and bimetallic nanoparticles in aqueous medium (A) (a-Ag, b-Cu-Ag (1:3), c-Cu-Ag(1:1), d-Cu-Ag (3:1), e-Cu); the distribution of particle size (B) of Ag (a), Cu-Ag (1:1) (b), and (c) Cu

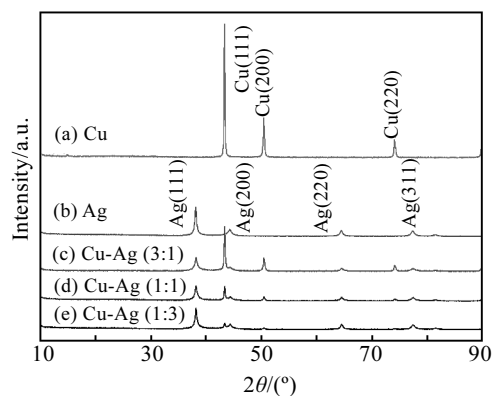


Fig.8 XRD patterns of Cu, Ag, Cu-Ag (3:1), Cu-Ag (1:1) and Cu-Ag (1:3)

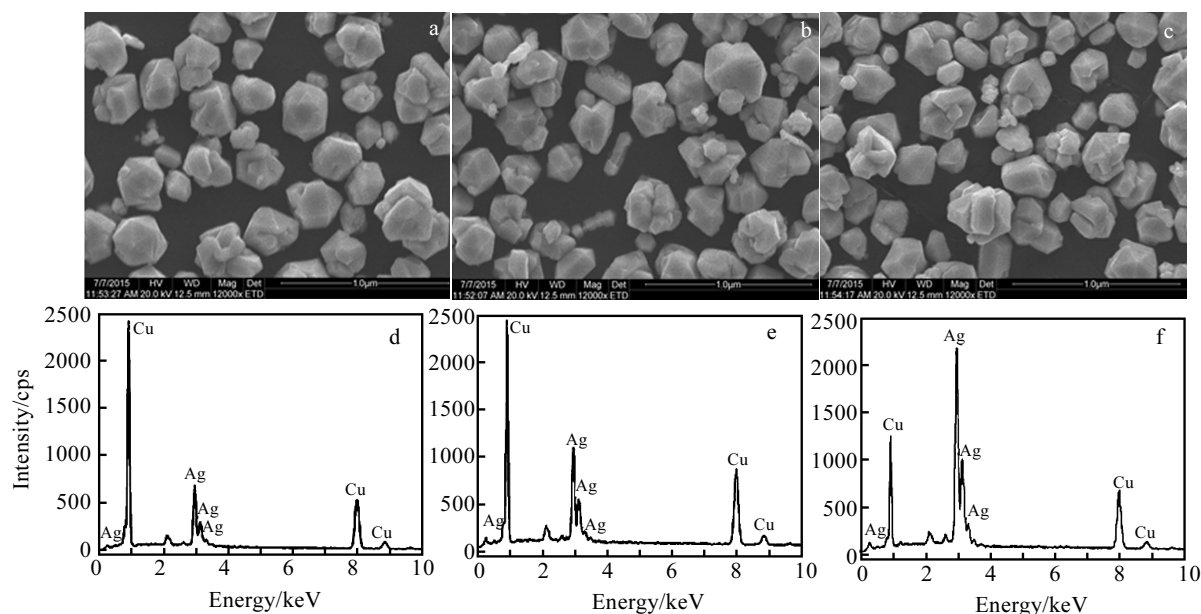


Fig.9 SEM images for Cu-Ag (3:1) (a), Cu-Ag (1:1) (b), Cu-Ag (1:3) (c); EDX spectra for Cu-Ag (3:1) (d), Cu-Ag (1:1) (e), Cu-Ag (1:3) (f)

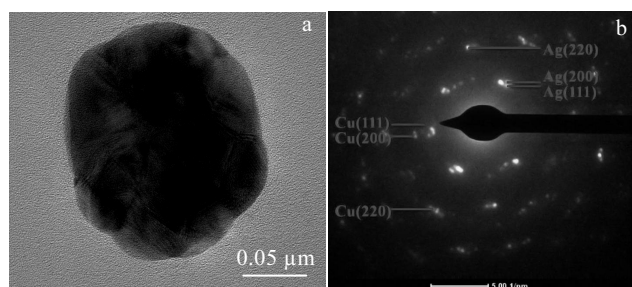


Fig.10 TEM image (a) and selected area electron diffraction pattern (b) of Cu-Ag (1:1)

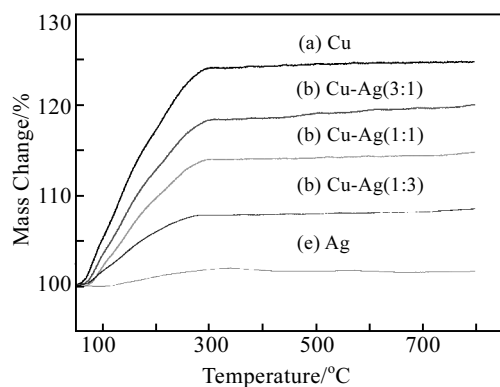


Fig.11 TGA curves of Cu, Cu-Ag (3:1), Cu-Ag (1:1), Cu-Ag (1:3), and Ag nanoparticles

respectively, as can be seen in Fig.11b~11d. There is no obvious increase in mass for pure silver, indicating that the silver has good thermal stability<sup>[34]</sup>. From above analysis, it can be concluded that the Cu-Ag alloy has better thermal stability than pure copper.

### 3 Conclusions

- 1) Cu-Ag nanoparticles with different molar ratios are prepared using hyperbranched polyester as the template.
- 2) The diameter of the Cu-Ag alloy particles are around 120 nm with a narrow size distribution. The Cu-Ag alloy particles prepared by this method have potential application in many fields, such as microelectronics, imaging materials, information storage materials, photoresist.

**Acknowledgments:** This work was supported by College Students Innovation and Entrepreneurship Training Program of Qilu University of Technology.

### References

- 1 Bastús N G, Merkoçi F, Piella J *et al. Chemistry of Materials*[J], 2014, 26: 2836
- 2 Wu J, Zan X, Li S *et al. Nanoscale*[J], 2014, 6: 749
- 3 Taner M, Sayar N, Yulug I G *et al. Journal of Materials Chemistry*[J], 2011, 21: 13150
- 4 Xiong J, Wang Y, Xue Q *et al. Green Chemistry*[J], 2011, 13: 900
- 5 Tan K S, Cheong K Y. *Journal of Nanoparticle Research*[J], 2013, 15: 1
- 6 Chen Z, Mochizuki D, Maitani M M *et al. Nanotechnology*[J], 2013, 24: 265 602

- 7 Singh M, Sinha I, Mandal R K. *Materials Letters*[J], 2009, 63: 2243
- 8 Momin T, Bhowmick A. *Journal of Alloys and Compounds*[J], 2013, 559: 24
- 9 Han Q, Chen X, Niu Y *et al.* *Langmuir*[J], 2013, 29: 8402
- 10 Zhang D, Li J, Chen S *et al.* *Macromolecular Chemistry and Physics*[J], 2013, 214: 370
- 11 Zhang H, Patel A, Gaharwar A K *et al.* *Biomacromolecules*[J], 2013, 14: 1299
- 12 Sun C, Chen X, Han Q *et al.* *Analytica Chimica Acta*[J], 2013, 776: 17
- 13 Jiang W, Zhou Y, Yan D. *Chemical Society Reviews*[J], 2015, 44: 3874
- 14 Alfurhood J A, Sun H, Bachler P R *et al.* *Polymer Chemistry*[J], 2016, 7: 2099
- 15 Giussi J M, Azzaroni O, Hensel-Bielowka S *et al.* *Polymer*[J], 2016, 100: 227
- 16 Wei X, Kong X, Yang J *et al.* *Journal of Membrane Science*[J], 2013, 440: 67
- 17 Jin H, Huang W, Zhu X *et al.* *Chemical Society Reviews*[J], 2012, 41: 5986
- 18 Han W. *Polymer Composites*[J], 2013, 34: 156
- 19 Zhuang Y, Deng H, Su Y *et al.* *Biomacromolecules*[J], 2016, 17: 2050
- 20 Wan D, Fu Q, Huang J. *Journal of Applied Polymer Science*[J], 2006, 101: 509
- 21 Li G, Luo Y. *Inorganic Chemistry*[J], 2008, 47: 360
- 22 Han W, Lin B, Yang H *et al.* *Designed Monomers and Polymers*[J], 2013, 16: 67
- 23 Han W, Lin B, Yang H *et al.* *Journal of Applied Polymer Science*[J], 2013, 128: 4261
- 24 Murillo E A, Vallejo P P, Sierra L *et al.* *Journal of Applied Polymer Science*[J], 2009, 112: 200
- 25 Huang H, Yang X. *Carbohydrate Research*[J], 2004, 339: 2627
- 26 Choi H, Lee J P, Ko S J *et al.* *Nano Letters*[J], 2013, 13: 2204
- 27 Valodkar M, Modi S, Pal A *et al.* *Materials Research Bulletin*[J], 2011, 46: 384
- 28 El-Daly A A, Fawzy A, Mansour S F *et al.* *Journal of Materials Science- Materials in Electronics*[J], 2013, 24: 2976
- 29 Raju K S, Sarma V S, Kauffmann A *et al.* *Acta Mater*[J], 2013, 61: 228
- 30 Wang M, Averbach R S, Bellon P *et al.* *Acta Materialia*[J], 2014, 62: 276
- 31 Kanagaraj J, Panda R C, Sumathi V. *RSC Advances*[J], 2015, 5: 45300
- 32 Xu H, Van Deventer J S J. *Cement and Concrete Research*[J], 2002, 32: 1705
- 33 Singh M, Shpargel T P, Asthana R. *Journal of Materials Science*[J], 2008, 43: 23
- 34 Sun L, Zhang Z, Dang H. *Materials Letters*[J], 2003, 57: 3874

## 用简便方法以超支化聚酯为模板合成 Cu-Ag 合金

韩文松

(齐鲁工业大学(山东省科学院)先进能源材料研究所, 山东 济南 250353)

**摘要:** 以超支化聚酯为模板, 用抗坏血酸为还原剂合成了不同摩尔比的 Cu-Ag 粒子。用第 1 代超支化聚酯为核, 2, 2-二羟甲基丙酸为支化单体, 通过逐步聚合反应合成了第 3 代的超支化聚酯。合成的超支化聚酯和 Cu-Ag 合金用红外光谱 (FT-IR), 核磁共振谱 ( $^1\text{H-NMR}$ ), 紫外光谱 (UV-vis), X 射线衍射 (XRD), 能量分散 X 射线分析 (EDX) 和激光粒度分析等手段进行表征。XRD 和 EDX 研究确认了 Cu-Ag 合金的形成。激光粒度仪, 扫描电镜 (SEM) 和透射电镜 (TEM) 研究表明 Cu-Ag 合金的平均粒径为 120 nm, 并且具有很好的分散性。热性能用热重分析 (TGA) 进行了表征, 结果显示测量值和理论值相近。

**关键词:** 稀有金属; Cu-Ag 合金; 超支化聚酯; 合成

---

作者简介: 韩文松, 男, 1973 年生, 博士, 齐鲁工业大学化学与制药工程学院, 山东 济南 250353, E-mail: hws0633@163.com